

Diabatic States, Couplings and Potential Energy Surfaces through the Block Localized Excitation Method

Peng Bao,^{*,†} Qiang Shi,^{*,†,‡} and Jiali Gao^{*,¶,§}

[†]*Beijing National Laboratory for Molecular Sciences, State Key Laboratory for Structural Chemistry of Unstable and Stable Species, CAS Research/Education Center for Excellence in Molecular Sciences, Institute of Chemistry, Chinese Academy of Sciences, Zhongguancun, Beijing 100190, China*

[‡]*University of Chinese Academy of Sciences, Beijing 100049, China*

[¶]*Shenzhen Bay Laboratory, and Lab of Computational Chemistry and Drug Design, Peking University Shenzhen Graduate School, Shenzhen, 518055, China*

[§]*Department of Chemistry and Supercomputing Institute, University of Minnesota, Minneapolis, Minnesota 55455, United States*

E-mail: baopeng@iccas.ac.cn; qshi@iccas.ac.cn; gao@jialigao.org

Abstract

We propose a new block localized excitation (BLE) method to directly construct diabatic excited states without the need to first compute the adiabatic states. The new method is capable to keep any electrons, spins, and excitations localized in any divided blocks of intermolecular and intramolecular systems. At the same time, the electrostatic, exchange, and polarization interactions between different blocks can be fully taken account of. To achieve this, a new Δ SCF project method and the maximum

wavefunction overlap method are employed to obtain localized excited states with orbitals relaxation, and the coupling between them are obtained using approaches similar to the multistate DFT (MSDFT) method. Numerical results show that the new BLE method is accurate in calculating the electronic couplings of the singlet excitation energy transfer (SEET) and triplet energy excitation transfer (TEET) processes, as well as the excited-state intermolecular potential energy surface.

1 Introduction

Modern computational quantum chemistry usually starts with solving the electronic Schrödinger equation within the Born–Oppenheimer (BO) approximation.¹ The resulted ground and excited states are adiabatic states as they are the eigenstates of the electronic Hamiltonian with fixed nuclear positions. In cases where the BO approximation holds, the adiabatic states provide good descriptions of the molecular structure and interaction. There are cases where the BO approximation becomes invalid, typical examples include excited state dynamics near avoided crossings or conical intersections,^{2–4} as well as problems of electron transfer (ET) and excitation energy transfer (EET) reactions.⁵ Many of these problems are not easily handled using adiabatic states: Calculations of the non-adiabatic couplings involve derivatives of the wave functions, and the derivative coupling terms may often become singular at the crossing points.

In contrast to the adiabatic states, diabatic states keep their physical characters as the nuclear positions change, and the potential energy surfaces are smooth.^{2–4} Moreover, the coupling between diabatic states does not involve the derivative coupling terms due to the nuclear kinetic energy operator. Usually, strict diabatic states cannot be obtained,⁶ and many different methods are developed to construct approximate diabatic states.^{7–10} These methods can be classified into two different categories. The first category of methods are based on transformations from adiabatic states. This class of methods can get good results, but the computational costs are relatively high.^{7,9,10} In the second category of methods,

diabatic states are constructed directly by keeping their localized character.⁹ There are different methods to directly construct diabatic states in the literature. For example, the symmetry-broken method based on the unrestricted Hartree-Fock (UHF)^{11,12} is found to yield good results with a low computational cost. But they are usually limited to singlet and triplet ground states and it may be difficult to converge to the localized states.^{7,8}

A different class of methods that attract many recent interests construct the diabatic states based on the concept of fragmental electron constraints. Among them, the constrained DFT (CDFT) method is based on fragmental population constraints. The diabatic states are constructed by CDFT through constraining the sum of electron density to specific numbers in a certain domain,¹³⁻¹⁵ and a Lagrange multiplier is added to the whole Kohn-Sham potential in CDFT.¹³⁻¹⁵ CDFT can also be used to estimate ET and triplet excitation energy transfer (TEET) couplings (Ref. 15 and references there in). Recently, CDFT was employed with non-Aufbau occupation of the orbitals by the Δ SCF method to construct localized singlet excited state in singlet fission.¹⁶ One problem of CDFT is that, the fragment domains need be selected carefully with different population analysis methods since there is no exact partition. Also, although the electron number in a certain domain can be constrained, some electrons may not be localized in the specific domain, which may lead to error diabatic states.¹⁷ Subsystem DFT, or frozen DFT, is the another method based on fragmental orbital constraints. The diabatic states are constructed through adding embedding potential to Kohn-Sham potential of fragmental SCF.¹⁸⁻²⁰ Because of the approximation of the non-additive part of the kinetic energy, Subsystem DFT is usually applied to weakly interacting system.^{20,21}

The valence bond (VB) theory naturally has the form of orbital constraints. In the VB theory, the reactant and product states and other resonance structures are represented by diabatic states.²²⁻²⁶ The *ab initio* VB theory is an appropriate method to construct diabatic states,²⁶⁻³³ but it can not handle the large number of VB configurations for large and condensed phase systems.²⁶ To combine the advantages of the molecular orbital (MO) theory

and the VB theory, a mixed molecular orbital and valence bond (MOVB) theory^{26,34–38} and its density functional theory (DFT) extension, the multistate DFT (MSDFT) method,^{21,39} were developed, based on a block-localized wavefunction (BLW) method^{40–42} and a similar block-localized DFT (BLDFT) method,⁴³ respectively. There are other similar self-consistent field (SCF) localized methods such as Stoll’s method,⁴⁴ the self-consistent field for molecular interactions (SCF-MI),^{45–47} locally projected MO (LPMO),^{48,49} localized MOs (ALMOs),^{50,51} and the gradient method with respect to orbital coefficients.^{31,44,52–54}

In the MOVB and MSDFT methods, the MOs and electrons are strictly localized in the individual fragments in a diabatic state. Therefore, the block-localized method can be considered as orbital constraints method. There is no charge transfer but electrostatic, exchange and polarization between different fragments. The energy of the localized electronic state is variationally minimized through SCF or direct minimization using gradient with respect to orbital coefficients. Therefore, the block-localized method is computationally inexpensive. Recently, the block-localized diabatic state are applied in many areas, mostly for ground state calculations in individual fragments,^{21,39,55,56} including two triplet ground state with opposite spin in the recent study of singlet fission.⁵⁷ To obtain localized excited states, several methods were developed. The simplified approach is to directly combine wavefunctions of individual fragments.⁵⁸ This approach ignores the interaction between individual fragments including electrostatic, exchange and polarization. A further simplified approach is the combination of the frontier orbitals of individual fragments.^{59,60}

In this work, we extended the block-localized methods to treat electronic states that involve excited states in individual fragments. Similar to previous works on ground states, the main focus is to obtain localized excited states for a given fragment. In principle, such calculations can be done using the inexpensive TDDFT⁶¹ and the single excitation configuration interaction (CIS) methods. But the TDDFT and CIS are multi-configuration methods that makes the following MSDFT calculations more complicated.

We thus resort to single configuration methods and employ the Δ SCF method⁶² as the

underlying method to construct localized excited states. One problem of the original Δ SCF method is that, the converged excited states may collapse to the ground state or other excited states. To solve this problem, the maximum overlap method (MOM),⁶³ and more recently, the maximum overlap square^{64,65} have been proposed. Once the single configuration localized excited states are obtained, further construction of the diabatic states are rather similar to the corresponding ground state MSDFT method.

The remainder of this paper is organized as follows. In section 2, we present the theory and computational details of the new BLE method. To obtain the single-reference locally excited state, we also propose a new and efficient Δ SCF project method. Numerical results are then presented in section 3, where we apply the new method to calculate SEET and TEET couplings for a model system, as well as excited state intermolecular interactions and excited state potential energy surface. Finally, conclusions and discussions are made in section 4.

2 Theory and Computational Method

2.1 Block-localized method for the ground state

For completeness, we begin with a brief review of methods based on molecular fragment or block localization, called block-localized wavefunction (BLW), for the ground electronic state calculations. Similar approaches will be used later to construct the diabatic states involving excited states. In BLW, the determinant wave function is written as follows:^{21,40,41,43}

$$\Psi_u = N_u \hat{A} \{ \Phi^1 \Phi^2 \dots \Phi^K \} \quad (1)$$

where N_u is the normalization constant, \hat{A} is the anti-symmetrization operator, K is the number of molecular fragments, or blocks, which could be a group of atoms, or a list of atomic orbital basis functions. In Eq. 1, Φ^A is a product of block-localized spin-orbitals,

$\Phi^A = \varphi_1^A \alpha \varphi_1^A \beta \dots \varphi_{n_{A\alpha}}^A \alpha \varphi_{n_{A\beta}}^A \beta$ in block A. The orbitals from different blocks are generally nonorthogonal since they typically do not share the same basis functions as a result of block fragmentation.⁴⁴ The block-localized molecular orbitals (BLMO) are linear combinations of atomic orbitals (LCAO) $\chi_{A\mu}$ within a specific block A:

$$|\varphi_i^A\rangle = \chi_A T_i^A = \sum_{\mu=1}^{m_A} |\chi_{A\mu}\rangle T_{\mu i}^A, \quad A = 1, 2, \dots, K \quad (2)$$

where block A consists of $n_A = n_{A\alpha} + n_{A\beta}$ electrons and m_A basis functions, and the MO coefficients are denoted as $T_{\mu i}^A$.

The total coefficient matrix T is block-diagonal when different blocks do not overlap, but in the present approach, different blocks can share a group of common basis functions. The total density matrix D is given by

$$D = T (T^\dagger S T)^{-1} T^\dagger \quad (3)$$

where $S = \chi^\dagger \chi$ is the overlap matrix of the atomic orbitals. The density matrix D defined above satisfies the symmetry ($D^\dagger = D$) and generalized idempotency ($DSD = D$) conditions.

The corresponding electron density is:

$$\rho = \chi D \chi^\dagger \quad (4)$$

In the HF theory, the electronic energy is given by

$$E = \text{Tr} [D (h + F)] \quad (5)$$

where h is the one-electron core Hamiltonian, and F is the Fock matrix. In KS-DFT, the electronic energy is

$$E = \text{Tr} (Dh) + \frac{1}{2} \text{Tr} (DJD) + E_{xc}(\rho) \quad (6)$$

where J is the Coulomb integral matrix, and $E_{xc}(\rho)$ is the exchange-correlation energy. The first-order variation of the energy with respect to the coefficient matrix T is given by:^{31,44,45,52-54}

$$\delta E = \text{Tr}(\delta D \cdot F) = 2\text{Tr} \left[(I - SD_\alpha) F_\alpha T_\alpha (T_\alpha^\dagger S T_\alpha)^{-1} \delta T_\alpha^\dagger + (I - SD_\beta) F_\beta T_\beta (T_\beta^\dagger S T_\beta)^{-1} \delta T_\beta^\dagger \right] \quad (7)$$

The energy gradients with respect to orbital coefficients can then be obtained using Eq. 7, based on which the Broyden-Fletcher-Goldfarb-Shanno (BFGS) updating scheme is used to optimize the BLMO.⁶⁶ The gradient optimization method can be applied to closed shell, restricted open shell, and unrestricted open shell cases. Both analytic orbital gradient and numerical orbital gradient have been implemented in our program. It is usually easy to get converged result when there is no common basis sets between different blocks. When there is overlap of basis sets between different blocks, it has been found previously that second order gradients methods using approximate Hessian further improve the convergence.^{53,54}

Three different forms of SCF equations have been described. In the first method, the whole system is first separated into two parts, the part that belongs to block A ($\rho_{\notin A}$), and the remainder of the system ($\rho_{\in A}$). The SCF equations for block A are then given by:^{21,42,43,45,48,49,67}

$$(1 - \rho_{\notin A}) f(1 - \rho_{\notin A}) \left| \varphi_i^A \right\rangle = (1 - \rho_{\notin A}) \left| \varphi_i^A \right\rangle \varepsilon_i^A, \quad (8)$$

which can also be written in matrix form

$$F'_A T_A = S'_A T_A E_A. \quad (9)$$

In Eq. 9 $F'_A = (I_{Na} - D_{\notin A} S_{Na})^\dagger F (I_{Na} - D_{\notin A} S_{Na})$ and $S'_A = S_{aN} (I_{Na} - D_{\notin A} S_{Na}) = S_{aa} - S_{aN} D_{\notin A} S_{Na}$ where I is the unit matrix, the subscript a denotes the basis functions of block A , the subscript N indicates full dimension of basis functions of the whole system, E is the

matrix of orbital energies, ε , the electron density operator $\rho_{\notin A}$ and the density matrix $D_{\notin A}$ describe the parts that does not belong to block A , which are defined as:

$$\rho_{\notin A} = \chi D_{\notin A} \chi^\dagger \quad (10)$$

$$D_{\notin A} = T_{\notin A} \left(T_{\notin A}^\dagger S T_{\notin A} \right)^{-1} T_{\notin A}^\dagger \quad (11)$$

In Appendix A, we also provide a more direct derivation and properties of Eq. 8.

The second method to obtain the localized orbitals in block A is to solve the eigenvalue problem by using a Hermitian operator ρ_A^x :^{46,50}

$$(1 - \rho + \rho_A^x) f(1 - \rho + \rho_A^x) |\varphi_i^A\rangle = (1 - \rho + \rho_A^x) |\varphi_i^A\rangle \varepsilon_i^A \quad (12)$$

where

$$\rho_A^x = \chi T \left[(T^\dagger S T)^{-1} \right]_{.A} \left[(T^\dagger S T)^{-1} \right]_A T^\dagger \chi^\dagger \quad (13)$$

In Eq. 12, $\rho = \rho_A^x + \rho_{\notin A}$ (Appendix A), the superscript A denotes the occupy orbitals of block A .

In the third method, the eigenvalue problem is solved by using a non-Hermitian operator ρ_A^s ,^{44,50}

$$(1 - \rho + \rho_A^{s \dagger}) f(1 - \rho + \rho_A^s) |\varphi_i^A\rangle = |\varphi_i^A\rangle \varepsilon_i^A \quad (14)$$

$$\rho_A^s = \chi T \left[(T^\dagger S T)^{-1} \right]_{.A} T_A^\dagger \chi^\dagger \quad (15)$$

The three methods are derived from the equation of zero energy gradient, and their computational costs are essentially the same when the number of the blocks is not large. In this work, the first method is used for the ground state calculations, and is extended to the localized orbitals for excited states (below).

To accelerate the convergence of the SCF, we employ the direct inversion in the iterative subspace (DIIS) method⁶⁸ by using the energy gradients (Appendix A) as the error vectors

and updating the projected Fock matrix and the effective overlap matrix for each block. We have also implemented a DIIS by updating the Fock matrix and coefficients of the whole system. Efficiencies of the two methods are found to be similar.

2.2 Block-localized excitation

The structure of the BLE method is similar to that presented in the previous subsection for the ground state, the main difference is that we need to obtain the localized excited state of a block, for example, block A, using a set of localized orbitals. Traditional excited state methods are usually of multi-configurational nature, even for the simplest excited state methods such as CIS and TDDFT. Using a multi-configurational wave function in one block to represent local excitation states brings more complexity to the block-localized algorithm presented in the previous subsection. To avoid this problem, we employ the Δ SCF like method,⁶² which is a single configuration excitation method, to construct the localized orbitals and the locally excited states, such that the framework presented in section 2.1 can be preserved in the BLE method.

The Δ SCF method solves the localized orbitals in a way that is very similar to the ground state Hartree-Fock-Roothaan equation. It is known that the original Δ SCF method⁶² often suffers from SCF convergence, and when it converges, an unwanted excited state, or the ground state could be obtained. One reason for the difficulty is due to the use of an identical order to permute occupied and virtual orbitals in each SCF iteration. However, the order of orbitals may have changed during the SCF from the initial guess. The convergence can be greatly improved by using the maximum overlap method (MOM),⁶³ and SCF convergence could be further improved by using maximum overlap squared.⁶⁴

A number of local excitation Δ SCF methods have been reported,^{69–84} including the local SCF method for core-excited states⁷⁰ and a constricted variational DFT (SCF-CV-DFT) by one electron excitation to the virtual orbital space.⁷¹ The single determinant approach can also be achieved by orthogonality constraints on the excited state. The “big shift” method

was formulated by setting a large value (more than 10^{10} a.u.) to the diagonal element of the Fock matrix corresponding to ground state orbitals.⁷² Similarly, an asymptotic projection method was suggested by adding a infinite projector to the frozen orbital in the Hamiltonian operator.⁷³ A yet another alternative is the guided SCF approach by transformation of the Fock matrix from the atom orbitals (AO) basis to the excited state orbitals basis.⁷⁴ Similar to the BLW method, but enforcing orbital orthogonality between core and valence, or between different fragments,,⁷⁶ is the projection configuration interaction method.⁷⁷

In this work, we adopt the Δ SCF approach and employ two techniques to ensure SCF convergence. In the first method, we first project the Δ SCF equations to the orbitals of the ground state space in each iteration. As an example, we study the case where one α orbital is excited. The ground state wavefunction is obtained from HF or DFT, by solving the Hartree-Fock-Roothaan equation iteratively:

$$F^0 T^0 = S T^0 E^0 \quad (16)$$

The optimized ground state α orbitals are $|\varphi_{1\alpha}^0 \varphi_{2\alpha}^0 \dots \varphi_{i\alpha}^0 \dots \varphi_{n\alpha}^0 \dots \varphi_{i'\alpha}^0 \dots \varphi_{m\alpha}^0\rangle$, where i denotes hole orbital (an occupied orbital), i' denotes particle orbital (an unoccupied orbital), $n\alpha$ is the number of α electrons and m is the basis size. If we want to obtain the α excitation $\varphi_{i\alpha} \longrightarrow \varphi_{i'\alpha}$, the initial guess for orbitals of the excited state is the $i \longleftrightarrow i'$ permutation of the ground state α orbitals, $|\varphi_{1\alpha}^0 \varphi_{2\alpha}^0 \dots \varphi_{i'\alpha}^0 \dots \varphi_{n\alpha}^0 \dots \varphi_{i\alpha}^0 \dots \varphi_{m\alpha}^0\rangle$, and there is no permutation of the β orbitals.

By using the above initial guess, we start from the unrestricted open shell Hartree-Fock-Roothaan SCF equation

$$f |\varphi\rangle = |\varphi\rangle \varepsilon \quad (17)$$

To solve this equation, we set $|\varphi\rangle = \chi T = \chi T^0 T'$, and left multiply $\langle \varphi^0 | = (\chi T^0)^\dagger$ to obtain

the matrix form of (Eq. 17) in the ground state MO basis. We have

$$(T^{0\dagger}FT^0)T' = (T^{0\dagger}ST^0)T'E \quad (18)$$

It is note that $T^{0\dagger}ST^0 = I$ without localized constraint, but it is not orthogonal in a localized block. After solving the eigenstate problem by using Jacobi diagonalization, we obtain eigenvector T' with order $\{12\dots i\dots n\dots i'\dots m\}$. It is note that, after solving the eigenstate problem, the eigenvectors are not sorted according to the energy of each orbitals as in the conventional SCF calculation. We then reorder T' to $T'_{i\leftrightarrow i'}$ with order $\{12\dots i'\dots n\dots i\dots m\}$ to construct the Fock matrix to realize Δ SCF excitation, i.e., $T_{new} = T^0T'_{i\leftrightarrow i'}$ in AO basis is used to do the next iteration. Alternatively, we can also use a permuted T^0 to realize the Δ SCF excitation, then follow above process without eigenvector permutation. Usually, good convergence can be obtained by using projection of ground state orbitals. We can also use the orbitals produced in previous iteration to do projection as a backup.

In a similar way, we can do any α and β excitation including multi-excitation through Δ SCF project method. We note that the guided SCF method⁷⁴ also employ a similar projection method. The method presented above is not orthogonal, but the overlap between ground state and excited state is usually very small. To obtain orthogonal excited state, the particle orbital can be obtained from the projection of unoccupied orbital space after obtaining hole orbital from full space projection. Similar to the derivation for the block-localized formalism, the detail derivation within localized constraint is presented in the Appendix A. In comparison, the hole orbital is obtained only from the occupied orbital space in the EHP method.^{79,80}

Another method to improve the convergence of the original Δ SCF method is based on the idea of maximum wavefunction overlap with an initial guess of an excited state Slater determinant. We also take one α orbital excitation as example. Like the Δ SCF project method presented above, we first obtain an initial guess of the single reference excited

state, by using the $i \longleftrightarrow i'$ permutation of the ground state α occupied orbitals, $\Phi^{0e} = |\varphi_{1\alpha}^0 \varphi_{2\alpha}^0 \dots \varphi_{i'\alpha}^0 \dots \varphi_{n\alpha}^0\rangle$, (the occupied β orbitals are kept unchanged). The overlap integral of the new wavefunction Φ and Φ^{0e} is

$$\langle \Phi^{0e} | \Phi \rangle = |T^{0e\dagger} ST| = \begin{vmatrix} O_{1^{0e}1} & \dots & O_{1^{0e}n} \\ \vdots & \ddots & \vdots \\ O_{n^{0e}1} & \dots & O_{n^{0e}n} \end{vmatrix} \quad (19)$$

where T^{0e} and T are the initial and new occupied orbital coefficients, respectively, O_{ij} is the orbital overlap integral. To obtain the maximum overlap between Φ^{0e} and Φ , we need to select n occupied orbitals from m total ones after diagonalization. In principle, we can calculate all different overlap integrals, and choose the combination with the maximum overlap. But the total number of overlap calculations would be too big (C_m^n). A small active space of the hole and particle orbitals can be chosen in practice. Otherwise, to simplify the problem, we consider the square of the overlap integral,

$$\langle \Phi^{0e} | \Phi \rangle^2 = \left| (T^{0e\dagger} ST)^\dagger (T^{0e\dagger} ST) \right| = \begin{vmatrix} \sum_i O_{i^{0e}1}^2 & \dots & \sum_i O_{i^{0e}1} O_{i^{0e}n} \\ \vdots & \ddots & \vdots \\ \sum_i O_{i^{0e}n} O_{i^{0e}1} & \dots & \sum_i O_{i^{0e}n}^2 \end{vmatrix} \quad (20)$$

The Frobenius norm of the above matrix is:

$$\|T^{0e\dagger} ST\|_F = \sqrt{\sum_i^n \sum_j^n O_{i^{0e}j}^2} \quad (21)$$

Therefore, to obtain the largest Frobenius norm, we select orbitals by choosing the highest n values of $\sum_i^n O_{i^{0e}j}^2$, $j = 1, 2, \dots, m$, this is just the maximum overlap square method.^{63,64} Obviously, this method ignores the off-diagonal matrix elements in the right of the (Eq. 20). To get better convergence, we can select orbitals by choosing the n biggest eigenvalues of $(T^{0e\dagger} ST)^\dagger (T^{0e\dagger} ST)$ where T is $m \times m$ dimension, just like the procedure to obtain na-

ture orbitals through the density matrix.

With the above Δ SCF project method and the maximum wavefunction overlap method, localized orbitals for excited states for a given block A can be obtained, and the formalism developed in the previous subsection 2.1 can then be extended to treat the excited state. In practical calculations, the block can be a molecular fragment, molecule, or supermolecule. Since single configuration is used, the Δ SCF method does not have TDDFT’s problem in some systems such as charge transfer excitation, core excitation and double excitation. Unrestricted open shell treatment is used in both Δ SCF project and the maximum wavefunction overlap method. They are found to give the same energy after the convergence. We thus use the block-localized Δ SCF project excitation method to do all calculations in the next section.

2.3 Diabatic excited states and the electronic coupling

The above obtained excited states with excitations localized within a block are diabatic states. As in previous application of the MSDFT method for ground state calculations,^{21,39,56} in order to obtain the adiabatic states, we need to compute the coupling between these local excited states. For a pair of diabatic states Ψ_u and Ψ_w calculated using the HF method, the electronic coupling element can be calculated as:^{35,85–88}

$$H_{uw} = \langle \Psi_u | H | \Psi_w \rangle = M_{uw} \left[\text{Tr} \left(D_{uw}^\dagger h \right) + \frac{1}{2} \text{Tr} \left(D_{uw}^\dagger J D_{uw} \right) - \frac{1}{4} \text{Tr} \left(D_{uw}^\dagger K D_{uw} \right) \right] = M_{uw} F_{uw} \quad (22)$$

where u and w denote the two diabatic states, F_{uw} is a ‘normalized’ Hamiltonian matrix element, M_{uw} is the overlap integral between the two diabatic states, which is calculated from the determinant of the orbital overlap matrix,

$$M_{uw} = \left| T_u^\dagger S T_w \right| \quad (23)$$

and the transition density matrix D_{uw} is defined as:

$$D_{uw} = T_w \left(T_u^\dagger S T_w \right)^{-1} T_u^\dagger \quad (24)$$

In calculating the above coupling elements, Löwdin first obtained the expression of Hamiltonian matrix element between two nonorthogonal Slater determinants with the first- and the second-order cofactors.⁸⁹ Then the biorthogonal orbitals and singular value decomposition were applied to simplify the calculation.^{90,91} The approach was further developed using density matrix and basis functions without integral transformation.^{35,85–88}

The coupling term is calculated using the correlation energies for the two diabatic states, which can also be approximated by the energy difference between BLDFT and that of Hartree-Fock theory using BLKS orbitals.^{21,56}

$$H_{uw} \approx H_{uw}^{KS} + \frac{1}{2} M_{uw}^{KS} \left[E_u(\rho_u) - E_u^{KS} + E_w(\rho_w) - E_w^{KS} \right] \quad (25)$$

In this approach, we do not have the problems of the transition density functional. We also derive a new approximate approach which can derive the above result and another similar coupling term in Appendix B. The numerical results from these approximate approaches are almost the same in all the examples presented in this work. All next calculation uses Eq. 25. There is also another transition density functional approach described in Supporting information.

After all the Hamiltonian matrix elements H_{uw} and overlap matrix elements M_{uw}^{KS} are obtained, we can calculate the adiabatic states within the MSDFT framework, by solving the secular equation,

$$HC = MCE \quad (26)$$

Obviously, the MSDFT method obtains the dynamic correlation first and the static correlation at a later stage. It is thus different from CASPT2, where the static correlation are

obtained first and the dynamic correlation are treated later. The MSDFT method also has the advantages that, a much smaller number of configurations are needed, and the computational cost is at the DFT level.

Within the MSDFT framework, electronic coupling between the diabatic states can also be calculated.^{21,56} This is especially useful in calculating the coupling constants in the electron transfer and excitation energy transfer processes.⁵ The effective coupling term H'_{uw} between the u and w states can be calculated conveniently through Löwdin’s orthogonalization,

$$H'_{uw} = \frac{H_{uw} - M_{uw}(H_{uu} + H_{ww})/2}{1 - M_{uw}^2} \quad (27)$$

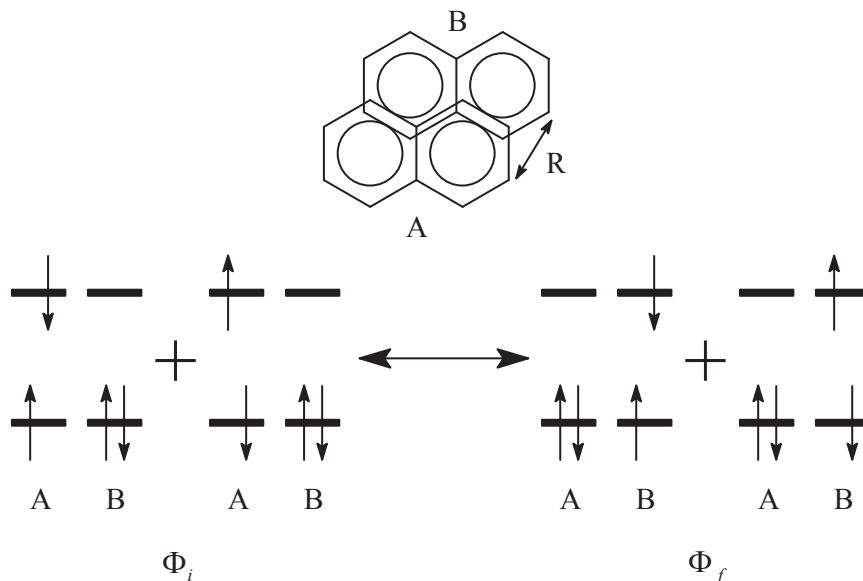
All the methods presented in this section are implemented in a modified version of GAMESS(US).⁶⁵

3 Results and discussion

As stated above, one of the important applications of the block-localized excitation (BLE) method presented above is to calculate the electronic coupling in the excitation energy transfer (EET) process, in which the electronic excitation energy is transferred from one part of the molecular system to another part.⁹² The EET process plays an important role in many artificial and natural molecular systems such as organic light-emitting diodes, photovoltaics, and photosynthetic system.^{93–98} In the weak coupling limit, the EET rate constant can be calculated using the Fermi’s golden rule:^{8,99}

$$k_{EET} = \frac{2\pi}{\hbar} |V|^2 \delta(E_i - E_f) \quad (28)$$

where V is the electronic coupling, E_i and E_f are the energy of the initial and final states, respectively. Therefore, the electronic coupling V is a key parameter to determine the EET rate constants. We apply the BLE method to calculate the EET couplings between



Scheme 1: The electronic configurations of HOMOs and LUMOs of the initial and final states in the SEET of the naphthalene dimer.

two face to face stacked naphthalene molecules (Scheme 1), which have been studied as a model system previously by using the combination of the frontier orbitals of individual fragments⁵⁹ and the fragment excitation difference (FED) method.¹⁰⁰ The D_{2h} geometry of the monomer was optimized at PBE0/6-31G* level in the ground state, as we have assumed that the diabatic electronic coupling constant does not change significantly with respect to the intramolecular degrees of freedom (i.e., the Frank-Condon approximation is applied for the coupling constant). All the calculations were carry out using unrestricted open shell at PBE0 level in a modified version of GAMESS(US).⁶⁵ In the BLE calculation, the dimer is separated into two blocks, *A* and *B*. Each block contains one naphthalene molecule, whose HOMO and LUMO orbitals are displayed in Scheme 1.

We first study the excitonic coupling in the singlet excitation energy transfer (SEET) of the 1^1B_{2u} excited state with HOMO to LUMO excitation. The separation between the two monomers ranges from 2.5 Å to 20 Å. According to Scheme 1, the localized initial singlet excited state, $\Psi_i = |A^*B\rangle$, is a spin-adapted excited state and linear combination

of the two localized excited states, $\Psi^{\alpha_A^*}$ and $\Psi^{\beta_A^*}$, obtained from the BLE method with the HOMO to LUMO excitation using the notation of the orbital wavefunctions. The final state $\Psi_f = |AB^*\rangle$ can be obtained in a similar way, such that,

$$\Psi_i = \frac{1}{\sqrt{2}} \left(\Psi^{\alpha_A^*} + \Psi^{\beta_A^*} \right) \quad (29)$$

$$\Psi_f = \frac{1}{\sqrt{2}} \left(\Psi^{\alpha_B^*} + \Psi^{\beta_B^*} \right) \quad (30)$$

The lowest excited state (1^1B_{2u}) is a $\pi \rightarrow \pi^*$ transition, which has obvious single reference character. We thus do not need more excited state configurations in calculating the coupling constant. Using symmetry simplification, Elements of the Hamiltonian and overlap matrices in Eq. 28 are then given by:

$$H_{ii} = \langle \Psi_i | H | \Psi_i \rangle = \langle \Psi^{\alpha_A^*} | H | \Psi^{\alpha_A^*} \rangle + \langle \Psi^{\alpha_A^*} | H | \Psi^{\beta_A^*} \rangle \quad (31)$$

$$H_{ff} = \langle \Psi_f | H | \Psi_f \rangle = \langle \Psi^{\alpha_B^*} | H | \Psi^{\alpha_B^*} \rangle + \langle \Psi^{\alpha_B^*} | H | \Psi^{\beta_B^*} \rangle \quad (32)$$

$$H_{if} = H_{fi} = \langle \Psi_i | H | \Psi_f \rangle = \langle \Psi^{\alpha_A^*} | H | \Psi^{\alpha_B^*} \rangle + \langle \Psi^{\alpha_A^*} | H | \Psi^{\beta_B^*} \rangle \quad (33)$$

$$M_{if} = \langle \Psi_i | \Psi_f \rangle = \langle \Psi^{\alpha_A^*} | \Psi^{\alpha_B^*} \rangle + \langle \Psi^{\alpha_A^*} | \Psi^{\beta_B^*} \rangle \quad (34)$$

The effective excitonic coupling for the SEET can then be obtained using Eq. 25 and Eq. 27. When the distance R between the two monomers is larger than 10 Å, the integral $\langle \Psi^{\alpha_A^*} | \Psi^{\alpha_B^*} \rangle$ is less than 10^{-8} because this is an exchange integral just like TEET. When the distance R between the dimers is larger than 2.5 Å, the integral $\langle \Psi^{\alpha_A^*} | \Psi^{\beta_B^*} \rangle$ and $\langle \Psi^{\alpha_A^*} | \Psi^{\beta_A^*} \rangle$ are less than 10^{-8} because one wavefunction is just the spin-flip of the other in the same or different block.

Figure 1 shows the excitonic coupling as a function of distance for the 1^1B_{2u} state. The results are similar to the ones obtained using the FED method.¹⁰⁰ At distances larger than about 6 Å, the excitonic coupling is proportional to the inverse of the cube of the distance,

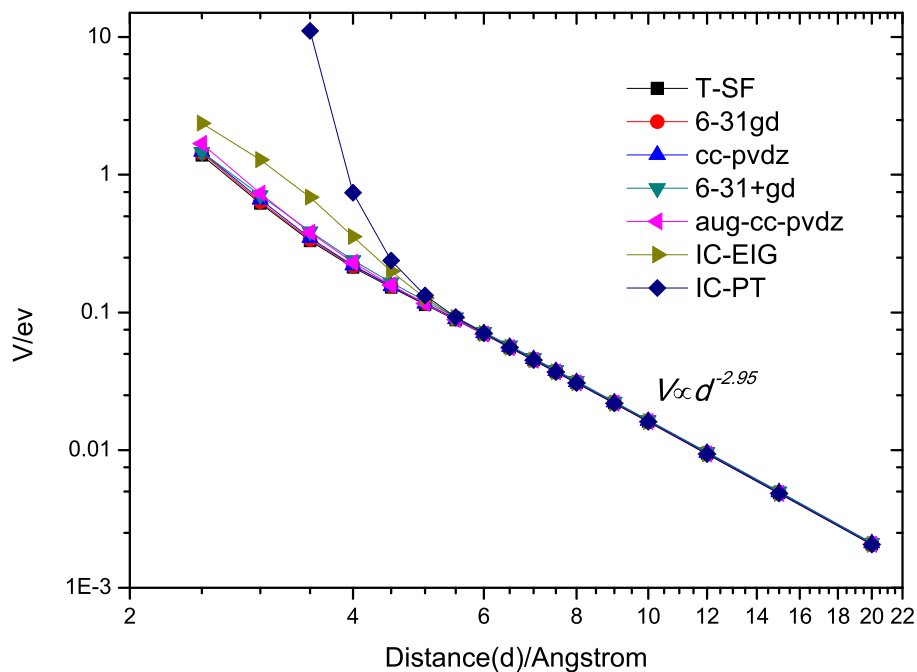


Figure 1: The SEET coupling as a function of the intermolecular distance for the 1^1B_{2u} state using PBE0 with different basis sets. T-SF means that the singlet diabatic wavefunctions are from spin-flip triplet block-localized wavefunctions ($M_s = 1$) with 6-31G* basis set. IC-PT means that the singlet diabatic wavefunctions include ionic configurations $|A^+B^- \rangle$ and $|A^-B^+ \rangle$ with the linear combination coefficients using the perturbation theory at aug-cc-pvdz level.¹⁰¹ IC-EIG means that the singlet diabatic wavefunctions include ionic configurations $|A^+B^- \rangle$ and $|A^-B^+ \rangle$ with the linear combination coefficients using eigen equation at aug-cc-pvdz level. The fitted slope was for the distances between 8-20 Å.

indicating that it is dominated by the long range coulomb coupling, in agreement with the Förster dipole-dipole interaction.^{8,100,102} At distances smaller than about 6 Å, the exchange coupling should also contribute to the total excitonic coupling. Different basis sets are used in the BLE calculation, and it can be seen that there is only small differences between the couplings calculated using different basis sets.

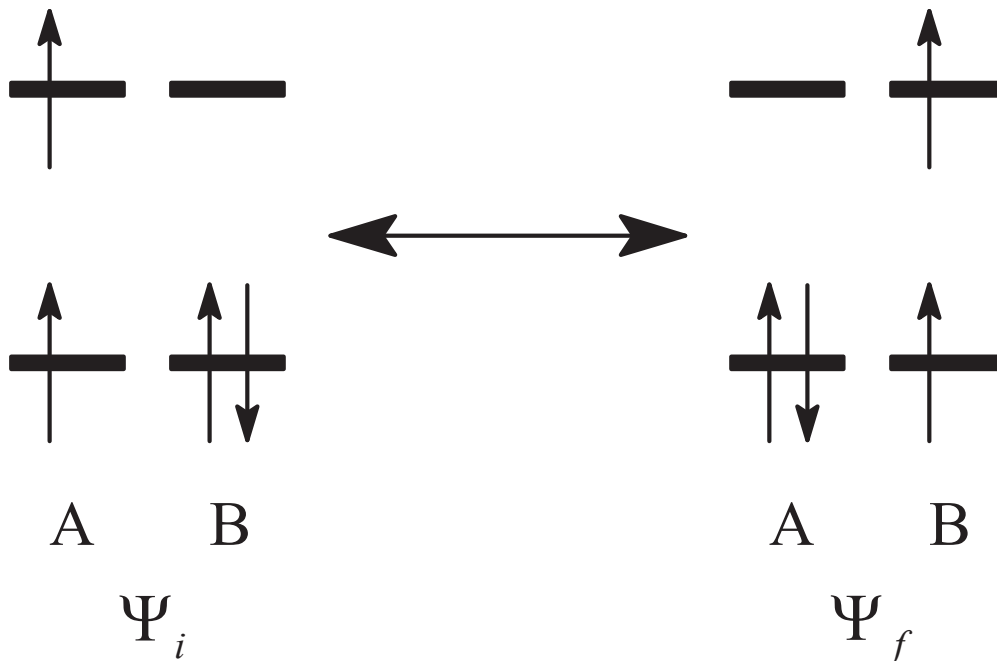
Further analyses of the SEET coupling are also performed in Figure 1. The curve labeled T-SF shows the case where the singlet diabatic wavefunctions are obtained from spin-flip of the triplet block-localized wavefunctions ($M_s = 1$) with 6-31G* basis set. The T-SF method gave the same couplings as the BLE method. The effect of ionic configurations (ICs) was also considered because the ICs can be the bridges from the initial to the final states. IC-PT means that the singlet diabatic wavefunctions include ionic configurations (ICs) $|A^+B^- \rangle$ and $|A^-B^+ \rangle$ with the linear combination coefficients using the perturbation theory at aug-cc-pvdz level.^{101,103,104} IC-PT can only work when the coefficients of ICs are small. Therefore, IC-PT should fail when the interaction between the two molecules is large or the two molecules are too close. To get exact effects of ICs, the eigen equation of initial and final states with ICs were also solved. IC-EIG means that the singlet diabatic wavefunctions include ionic configurations $|A^+B^- \rangle$ and $|A^-B^+ \rangle$ with the linear combination coefficients using eigen equation at aug-cc-pvdz level. Obviously, the excitonic couplings are overestimated by IC-PT method and underestimated by the BLE method without ICs at distances smaller than about 4 Å.

In contrary to the SEET, excitonic coupling in triplet excitation energy transfer (TEET) process of the 1^3B_{2u} excited state is dominated by short range coupling. According to Scheme 1, like the SEET case studied above, we can obtain two localized $M_s = 0$ triplet excited states with HOMO to LUMO excitation,

$$\Psi_i = \frac{1}{\sqrt{2}} (\Psi^{\alpha_A^*} - \Psi^{\beta_A^*}) \quad (35)$$

$$\Psi_f = \frac{1}{\sqrt{2}} (\Psi^{\alpha_B^*} - \Psi^{\beta_B^*}) \quad (36)$$

The excitonic coupling of TEET with $M_s = 1$ triplet states can also be obtained by using diabatic states constructed by the BLW method, which is shown in Scheme 2. For simplicity, the electronic configurations for the $M_s = 1$ states are not shown.



Scheme 2: The electronic configurations of HOMOs and LUMOs of the initial and final states in the TEET of the naphthalene dimer.

The calculated TEET excitonic couplings are shown in Figure 2 for both the $M_s = 0$ and $M_s = 1$ triplet states. We first compare the "1+1", "BLW", and "Relaxed" methods for $M_s = 1$ states and the BLE method for $M_s = 0$ states with the 6-31G* basis set. "1+1" means that the localized wavefunction is composed directly by the wavefunctions of two blocks. "Relaxed" means that the wavefunctions are relaxed without any restriction starting from BLW. The couplings of "Relaxed" method are the same starting either from BLW or "1+1". The couplings of "1+1", "BLW", and BLE methods have small differences because the polarization interaction between two blocks is small for the eclipsed naphthalenes at

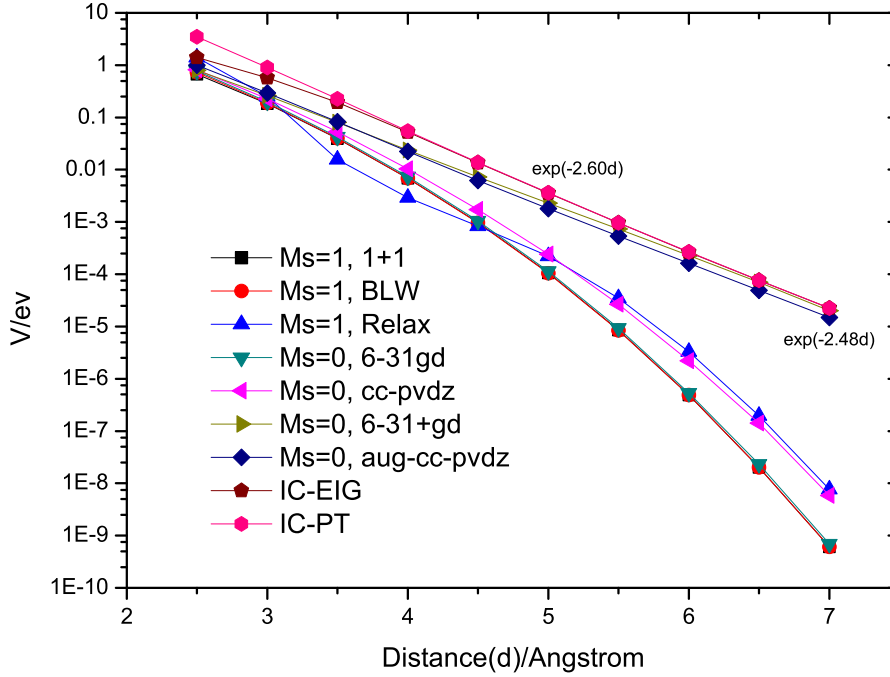


Figure 2: The coupling values vs. distances for the 1^3B_{2u} state using PBE0 with different basis sets. "1+1" means the localized wavefunction is composed directly by the wavefunctions of two blocks. "Relax" means the wavefunctions are relaxed without any restriction starting from BLW or "1+1". "1+1", "BLW" and "Relax" are all calculated with 6-31G* basis set. IC-PT means the triplet diabatic wavefunctions of $M_s = 0$ include ionic configurations $|A^+B^- \rangle$ and $|A^-B^+ \rangle$ with the linear combination coefficients using the perturbation theory at aug-cc-pvdz level.¹⁰¹ IC-EIG means the triplet diabatic wavefunctions of $M_s = 0$ include ionic configurations $|A^+B^- \rangle$ and $|A^-B^+ \rangle$ with the linear combination coefficients using eigen equation at aug-cc-pvdz level. the fitted exponents in the figures were obtained with ionic configuration IC-EIG (2.60\AA^{-1}) at distances of 3.5-7 \AA or without ionic configuration (2.48\AA^{-1}) at distances of 2.5-7 \AA .

certain distances. The "Relaxed" method did not give a smooth curve because the obtained wavefunction may deviate from the most optimized state when the distance is less than 4.5 Å. Therefore, The "Relax" method may not be stable when the interaction between two blocks are strong.

It is also shown in Figure 2 that, the TEET couplings are not affected by different diffusive basis sets 6-31+G* and aug-cc-pvdz which decay exponentially with perfect correlation. We can obtain the exponential decay of the TEET coupling with the distance $V_{TEET} \propto e^{-\beta r}$. The exponential decay constant of the TEET couplings β at aug-cc-pvdz level, 2.48 \AA^{-1} , is similar to the values found in Refs. 100,105. However, couplings calculated using small basis sets without diffusive functions decay faster than the ones with diffusive functions.

The ionic configurations are also found to have important effect on the TEET coupling even at the distance 7 Å, similar to the previous findings in Ref. 101,103,104. The couplings with ICs (IC-EIG and IC-PT) are about two times as the couplings without ICs. The exponent of the IC-EIG TEET couplings at aug-cc-pvdz level, 2.60 \AA^{-1} , is the same as the exponent in Ref. 100. Obviously, compare with IC-EIG, the excitonic couplings are overestimated by IC-PT method at distances smaller than about 3 Å. The exponential decay of the TEET coupling is similar to electron transfer coupling because the TEET can be viewed as two electron exchanges with different spin.⁷ We further calculated the couplings of electron transfer (ET) and hole transfer (HT) at aug-cc-pvdz level from 3.5 to 7 Å using MSDDFT for two naphthalene molecules. The β values of ET and HT are 1.00 and 1.45 \AA^{-1} , respectively. Thus, the β value of TEET is almost the sum of the β values of ET and HT.

According to Eqs. 22 and 27, when the overlap is small, the TEET coupling can be simplified to

$$H'_{uw} = \frac{M_{uw}}{1 - M_{uw}^2} (F_{uw} - H_{uu}/2 - H_{ww}/2) \approx M_{uw} C_{uw} \quad (37)$$

Because the density or the orbital coefficients change slowly when varying the molecular geometry in the diabatic states, C_{uw} may be approximate to a constant. The approximation $H'_{uw} = C M_{uw}$ is first employed in the extended Hückel theory (EHT),¹⁰⁶ and was applied

in electron transfer recently.^{107–109} To evaluate the relationship between the TEET couplings and the overlaps for coupling values spanning many orders of magnitudes (the least squares method cannot have the contribution of small value points), the minimization of the statistical metric denoted exponential root-mean-square logarithmic error (ERMSLE) was used.^{109,110} This means all the values of $\frac{H'_{uw}}{M_{uw}C_{uw}}$ should be approximately equal to 1.

$$ERMLSE = \exp \left[\left\langle \left(\ln \frac{H'_{uw}}{M_{uw}C_{uw}} \right)^2 \right\rangle^{1/2} \right] \quad (38)$$

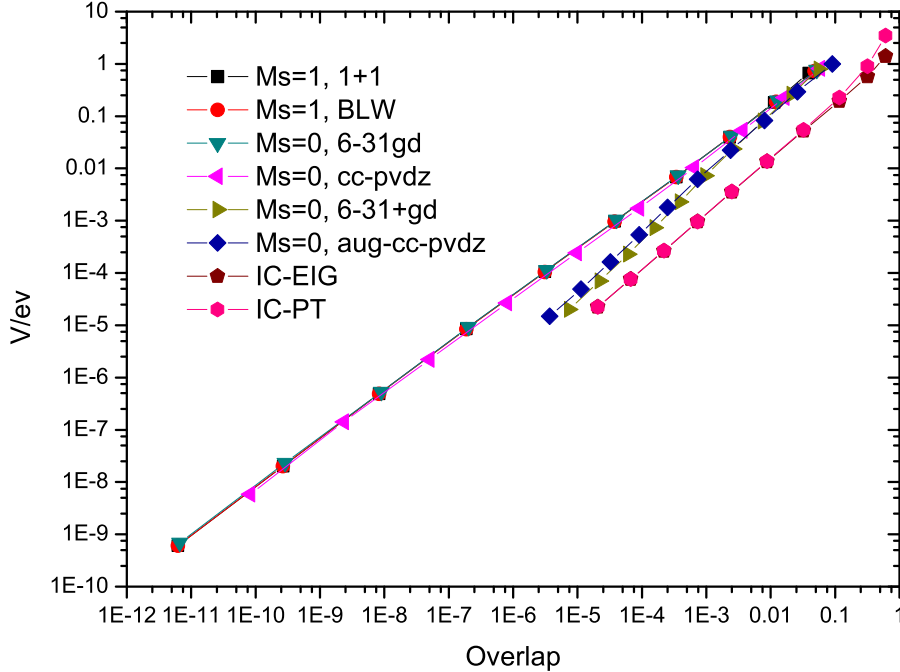


Figure 3: Correlations between the coupling constants and the wavefunction overlaps for TEET. The labels for all the curves are the same as those in Figure 2.

Figure 3 shows good linear correlation in the logarithmic scales between the excitation couplings and overlaps for the dimmer with the distances 2.5–7 Å. We obtain the C values (7.22eV, $R^2=0.992$, ERMSLE=1.4 for $M_s = 0$; 1.48eV, $R^2=0.994$, ERMSLE=1.2 for IC-EIG) at aug-cc-pvdz level. From Figure 3, we can also obtain a new relation $V = CM_{if}^x$

($V = 17.0M_{if}^{1.11}$ eV, $R^2=0.9994$, $M_s = 0$, aug-cc-pvdz; $V = 2.07M_{if}^{1.06}$ eV, $R^2=0.9997$, IC-EIG; $V = 10.5M_{if}^{0.908}$ eV, $R^2=0.9999$, $M_s = 0$, 6-31G*). The reason of the relation is that both coupling and overlap of the TEET decay exponentially with the distance.

The above calculations of SEET and TEET couplings concern Frenkel excitons, where the electron and hole are localized within the same block. The charge transfer states also play important roles in determining excited state properties. In the following, we apply the new BLE method to calculate the intermolecular interaction potential energy curve in the naphthalene excited dimer (excimer), where the exciton resonance state (ER, $A^*B \leftrightarrow AB^*$) and the charge resonance state (CR, $A^+B^- \leftrightarrow A^-B^+$) are the origin of the strongly attractive interaction.¹¹¹

Aromatic excimers, such as that formed between two naphthalenes, are often studied because of their typical photophysical and photochemical characters. With the development of computational chemistry, many different theoretical methods have been applied to study aromatic excimers, including the semiempirical,^{112,113} TDDFT,¹¹⁴ and post-SCF^{59,115,116} methods. In these works, the calculated properties of the excimer, such as binding energy, absorption energy, and emission energy, were found to heavily depend on the methods and basis sets. Up to date, the most advanced method to calculate the naphthalene excimer is the DMRG-CASPT2 (the density matrix renormalization group-the complete active space second order perturbation theory) approach using the full π valence orbitals as the active space, because of strong static and dynamic correlation.¹¹⁶ In comparison, the block-localized excited MSDFT (BLE-MSDFT) is much less computationally demanding, and is much easier to be applied to larger systems.

To calculate the intermolecular interaction in the excimer state, we use all the localized and charge-transfer states through HOMO-LUMO singlet excitation to construct ER and CR states. The singlet/triplet excited states are then determined as combinations of ER and CR states using the MSDFT method. The potential energy surface (PES) is shown in Figure 4. DFT means the ground state energy using DFT. BLW means the localized

ground state energy using BLW. S1ER/T1ER means the excitonic-resonance states, the lowest singlet/triplet state energy of the CI of four localized singlet excited states ($\Psi^{\alpha_A^*}$, $\Psi^{\beta_A^*}$, $\Psi^{\alpha_B^*}$ and $\Psi^{\beta_B^*}$). S1CR/T1CR means charge-resonance states, the lowest singlet/triplet state energy of the CI of four singlet charge-transfer states. S1/T1 means the first singlet/triplet excited state, the lowest singlet/triplet state energy of the CI of four singlet localized excited states and four singlet charge-transfer states.

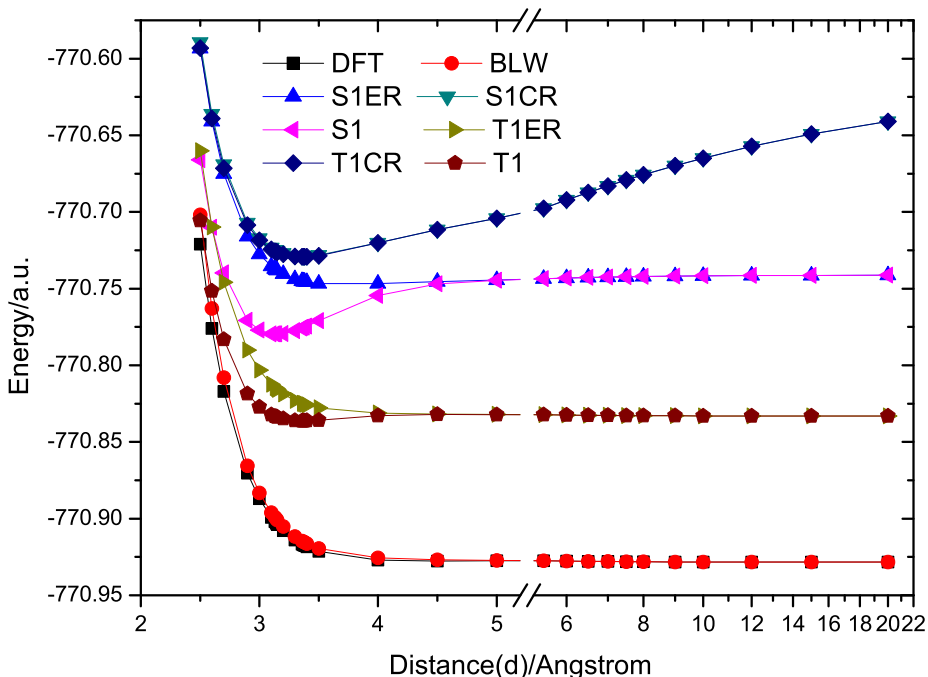


Figure 4: Potential energy curves of the ground and excited states of the naphthalene dimer using PBE0/cc-pvdz. DFT: the ground state energy using DFT; BLW: the ground state energy using BLW ; S1ER/T1ER: excitonic-resonance states, the lowest singlet/triplet state energy of the CI of four localized singlet excited states ($\Psi^{\alpha_A^*}$, $\Psi^{\beta_A^*}$, $\Psi^{\alpha_B^*}$ and $\Psi^{\beta_B^*}$); S1CR/T1CR: charge-resonance states, the lowest singlet/triplet state energy of the CI of four singlet charge-transfer states; S1/T1: the first singlet/triplet excited state, the lowest singlet/triplet state energy of the CI of four localized singlet excited states and four singlet charge-transfer states.

We first analyze the singlet states. The excimer state of the naphthalene is the lower state excited from HOMO to LUMO, named the L_a state.¹¹⁵ In contrast, for the monomer

of naphthalene, the L_b state, excited from HOMO to LUMO+1 and HOMO-1 to LUMO, is the lowest excited state, and the L_a state is the second lowest excited state.¹¹⁵ In present work, only the L_a excited state was considered when calculating the excimer properties.

With the increase of the intermolecular distance, the S1 and S1ER energies first decrease to a minimum and then increases. The S1ER state has a very small binding energy compare to S1 state, such that the S1CR states play an important role for the binding energy of the excimer state. As shown in Figure 4, the energy of the S1CR state clearly show the characteristics of the Coulombic interaction between two opposite ions at a distance larger than 4 Å.¹¹²

Table 1: Intermolecular Equilibrium Distance (r_e), Binding Energies (BE), and Transition Energies of the Naphthalene singlet state excimer. The numbers in parentheses are from BLW of ground state for eliminating BSSE.

Method	Basis set	r_e (Å)	BE (eV)	Transition energy (eV)	
				$r = r_e$	$r=20$ (Å)
BLE-MSPBE0	6-31G(d)	3.11	0.99	3.40(3.31)	5.16
BLE-MSPBE0	6-31+G(d)	3.19	1.07	3.36(3.28)	5.07
BLE-MSPBE0	cc-pVDZ	3.14	1.04	3.36(3.27)	5.09
BLE-MSPBE0	aug-cc-pVDZ	3.18	1.10	3.29(3.19)	4.99
BLE-MSPBE	cc-pVDZ	3.14	0.95	3.11(3.01)	4.75
BLE-MSB3LYP	cc-pVDZ	3.20	0.79	3.46(3.38)	5.03
BLE-MOVB	cc-pVDZ	3.35	0.91	4.23(4.17)	5.85
exptl.		3.0-3.6 ^a	0.76 ^{b, c}	3.13 ^b	4.45 ^c , 4.7 ^d

^a Ref. 117; ^b Ref. 112; ^c Ref. 118; ^d Ref. 119.

Table 1 presents the theoretical and experimental spectroscopic parameters of the naphthalene excimer state using different kinds of methods and basis sets. For the BLE-MSPBE0 method, the spectroscopic parameters show little basis set-dependent by using different basis sets 6-31G(d), 6-31+G(d), cc-pVDz and aug-cc-pVDZ. The intermolecular equilibrium distance, r_e , ranges from 3.11 to 3.19 Å, which is consistent with the experimental value and previous theoretical works.^{115–117} The binding energies, BE, ranges from 0.99 to 1.10 eV, is higher than the experimental value, and is consistent with the ground state BSSE (basis set superposition errors) corrected DMRG-CASPT2 values in Ref. 116. The transition energies

at the excimer structures, ranges from 3.29 to 3.40 eV, is very close to the experimental value. The transition energies at the superdimer structures, ranges from 4.99 to 5.16 eV, is slightly higher than the experimental value.^{118,119}

There is no BSSE by using BLW method because of separated basis sets.⁴⁵ Therefore, no BSSE is in the binding energies by using MSDFT calculation with same partition as monomers. The result in parentheses of the Table 1 is in line with this reason. At the equilibrium distance, the block-localized form eliminates the BSSE (0.11 eV/cc-pVDZ, 0.10 eV/aug-cc-pVDZ for the ground state) and is consistent with the BSSE (0.11 eV/cc-pVDZ, 0.10 eV/aug-cc-pVDZ for the ground state) by using the counterpoise procedure. In contrast, the basis set-dependence is quite obvious by using different basis sets from 6-31G(d) to aug-cc-pVDZ in Ref. 115. Similarly, all the spectroscopic parameters show little dependence on the density functionals in the BLE-MSDFT method (PBE, PBE0 and B3LYP) at cc-pVDZ level. In contrast, the density functional-dependence is obvious using different density functionals (PBE, PBE0 and B3LYP) in Ref. 114. The severe deviation between the values of BLE-MOVB and the experimental values indicates that the dynamic correlation is necessary for the intermolecular interactions in the excited states.

Then we analyze the triplet excited state of the naphthalene. There are still debates on the existence of the triplet naphthalene excimer from both experimental and theoretical studies.^{111,113,120-124} The PES of T1CR state is almost the same as the PES of S1CR state. The T1ER state energy decreases monotonously as the distance increases. Thus, the T1CR states play an important role when the distance between two parts is less than 4 Å. The T1 state potential energy curve has a minimum at around 3.4 Å, and a maximum at about 5 Å. There is 0.02-0.03 eV energy difference between the maximum energy at about 5 Å and the energy at 20 Å. The T1 state binding energy is about 0.1eV, which is much smaller than the S1 state binding energy.

Table 2 gave the experimental and theoretical spectroscopic parameters of the naphthalene dimers by using BLE-MSPBE0 method. The spectroscopic parameters are very less

Table 2: Intermolecular Equilibrium Distance (r_e), Binding Energies (BE), and Transition Energies of the Naphthalene triplet state excimer by using BLE-MSPBE0. The numbers in parentheses are from BLW of ground state for eliminating BSSE.

Basis set	r_e (Å)	BE (eV)	Transition energy (eV)	
			$r = r_e$	$r=20$ (Å)
6-31G(d)	3.39	0.02	2.29(2.21)	2.60
6-31+G(d)	3.45	0.07	2.26(2.20)	2.60
cc-pVDZ	3.37	0.08	2.21(2.15)	2.59
aug-cc-pVDZ	3.40	0.12	2.21(2.13)	2.59
exptl.			2.3 ^a	2.64 ^b

^a Ref. 120,121; ^b Ref. 125.

basis set-dependent by using different basis sets 6-31G(d), 6-31+G(d), cc-pVDz and aug-cc-pVDZ: the intermolecular equilibrium distance, r_e , ranges from 3.37 to 3.45 Å; the binding energies, BE, ranging from 0.02 to 0.12 eV, are very small to reflect the argument of forming the triplet excimer; the transition energies, 2.21-2.29 eV at equilibrium distance and 2.59-2.60 eV at 20 Å, are very close to the experimental value, 2.3 eV and 2.64 eV, respectively. The block-localized form eliminates the BSSE (0.08 eV/aug-cc-pVDZ for the ground state) and is consistent with the BSSE (0.08 eV/aug-cc-pVDZ for the ground state) by using the counterpoise procedure.

4 Conclusions

In summary, we have proposed an efficient BLE method, which combines the block-localized approach and the single configuration excitation method to directly construct diabatic excited states. Two new single configuration excitation methods, the Δ SCF project method and the maximum wavefunction overlap method are developed and implemented in the BLE method. Within in the framework of MSDFT, we show how the new BLE method can be applied to calculate the excitonic couplings in the SEET and TEET processes.

Numerical results show that the new BLE method is accurate in calculating the SEET and TEET coupling constants, and the excited state intermolecular interactions in aromatic

excimers. The calculated results also show little dependence on the choice of basis sets and density functionals. Although the calculations are performed on model systems consists of two identical monomers, the method can certainly be applied to heterodimers, molecular fragments, and possibly more complex molecular blocks. We thus expect that the new method can be applied to many problems of excited state structure and dynamics.

In the future, the BLE may be further simplified to use the Hartree product wavefunction between different blocks, such as the polarization of Morokuma energy decomposition analysis,¹²⁶ explicit polarized potential (X-pol),¹²⁷ fragment molecular orbital(FMO),¹²⁸ and restrict geometry optimization for aromaticity (RGO)¹²⁹ methods. The Hartree product wavefunction as diabatic state is accurate when the distance between two parts is large because the exchange and repulsion between two parts are small and the polarization effect is taken account of. It is also a linear scaling method for the large system, and can be applied to systems such as large molecular aggregates.

Acknowledgement

This work is supported by NSFC (Grant No. 21673246), and the Strategic Priority Research Program of the Chinese Academy of Sciences (Grant No. XDB12020300).

Appendix A Calculation of the block-localized ground and excited state energy gradients

The operator form of the ground state energy gradient of the equation 8 for RHF is given by:⁴⁴

$$\frac{\partial E}{\partial \langle \varphi_A |} = 4(1 - \rho)f |\tilde{\varphi}_A\rangle \quad (39)$$

where the reciprocal orbitals $|\tilde{\varphi}\rangle$ are

$$|\tilde{\varphi}\rangle = |\tilde{\varphi}_A \tilde{\varphi}_{\notin A}\rangle = |\varphi_A \varphi_{\notin A}\rangle \langle \varphi_A \varphi_{\notin A} | \varphi_A \varphi_{\notin A} \rangle^{-1} = |\varphi_A \varphi_{\notin A}\rangle \begin{pmatrix} \langle \varphi_A | \varphi_A \rangle & \langle \varphi_A | \varphi_{\notin A} \rangle \\ \langle \varphi_{\notin A} | \varphi_A \rangle & \langle \varphi_{\notin A} | \varphi_{\notin A} \rangle \end{pmatrix}^{-1} \quad (40)$$

Here in Eq. 40, $\langle \varphi | \varphi \rangle$ is the overlap matrix of the molecular orbitals, not an integral value.

By using the method of blockwise matrix inversion,¹³⁰

$$\begin{pmatrix} A & B \\ C & D \end{pmatrix}^{-1} = \begin{pmatrix} (A - BD^{-1}C)^{-1} & -(A - BD^{-1}C)^{-1}BD^{-1} \\ -D^{-1}C(A - BD^{-1}C)^{-1} & D^{-1}C(A - BD^{-1}C)^{-1}BD^{-1} + D^{-1} \end{pmatrix} \quad (41)$$

we set

$$\left(\langle \varphi_A | \varphi_A \rangle - \langle \varphi_A | \varphi_{\notin A} \rangle \langle \varphi_{\notin A} | \varphi_{\notin A} \rangle^{-1} \langle \varphi_{\notin A} | \varphi_A \rangle \right)^{-1} = \langle \varphi_A | (1 - \rho_{\notin A}) | \varphi_A \rangle^{-1} = \alpha \quad (42)$$

After some transformations, the following expressions are obtained

$$|\tilde{\varphi}\rangle = \left| (1 - \rho_{\notin A}) | \varphi_A \rangle \alpha, (1 - (1 - \rho_{\notin A}) | \varphi_A \rangle \alpha \langle \varphi_A |) | \varphi_{\notin A} \rangle \langle \varphi_{\notin A} | \varphi_{\notin A} \rangle^{-1} \right\rangle \quad (43)$$

$$\rho = |\tilde{\varphi}\rangle \langle \varphi_A \varphi_{\notin A} | = (1 - \rho_{\notin A}) | \varphi_A \rangle \alpha \langle \varphi_A | (1 - \rho_{\notin A}) + \rho_{\notin A} \quad (44)$$

$$\frac{\partial E}{\partial \langle \varphi_A |} = 4(1 - \rho) f |\tilde{\varphi}_A\rangle = 4(1 - (1 - \rho_{\notin A}) | \varphi_A \rangle \alpha \langle \varphi_A |) (1 - \rho_{\notin A}) f (1 - \rho_{\notin A}) | \varphi_A \rangle \alpha \quad (45)$$

We can further set α as a unit matrix to make $(1 - \rho_{\notin A}) | \varphi_A \rangle$ orthonormalized,

$$\alpha = \langle \varphi_A | (1 - \rho_{\notin A}) (1 - \rho_{\notin A}) | \varphi_A \rangle^{-1} = \langle \Phi_A | \Phi_A \rangle^{-1} = I \quad (46)$$

and obtain the energy gradient for block A ,

$$\frac{\partial E}{\partial \langle \varphi_A |} = 4(1 - (1 - \rho_{\notin A}) | \varphi_A \rangle \langle \varphi_A |) (1 - \rho_{\notin A}) f (1 - \rho_{\notin A}) | \varphi_A \rangle \quad (47)$$

At the point of the lowest energy, the energy gradient is zero. We obtain the SCF equation Eq. 9 with

$$\langle \varphi_A | (1 - \rho_{\notin A}) f (1 - \rho_{\notin A}) | \varphi_A \rangle = \varepsilon_A \quad (48)$$

Because α is a unit matrix, Eq. 44 now becomes

$$\rho = (1 - \rho_{\notin A}) | \varphi_A \rangle \langle \varphi_A | (1 - \rho_{\notin A}) + \rho_{\notin A} = \rho_A^x + \rho_{\notin A} \quad (49)$$

Eq. 12 can then be obtained by putting Eq. 49 into Eq. 9.

We have the property:

$$(1 - \rho_{\notin A}) | \varphi_{\notin A} \rangle = | \varphi_{\notin A} \rangle - \rho_{\notin A} | \varphi_{\notin A} \rangle = 0 \quad (50)$$

If we set $|\Phi_i^A\rangle = (1 - \rho_{\notin A}) |\varphi_i^A\rangle$, then $\langle \varphi_{\notin A} | \Phi_i^A \rangle = 0$. By multiplying $\langle \varphi_i^A |$ on the left of Eq. 8, using the idempotency relation $(1 - \rho_{\notin A})(1 - \rho_{\notin A}) = (1 - \rho_{\notin A})$, and keeping Φ_A orthogonal, we obtain:

$$\langle \Phi_i^A | f | \Phi_i^A \rangle = \langle \Phi_i^A | \Phi_i^A \rangle \varepsilon_i^A = \varepsilon_i^A \quad (51)$$

$$f | \Phi_i^A \rangle = \varepsilon_i^A | \Phi_i^A \rangle \quad (52)$$

The above derivation from Eq. 50 to Eq. 52 is a reversed process of generalized Phillips-Kleiman pseudopotential derivation in Ref. 75 . This means that the projected wavefunction of block A orthogonalized to all other blocks is the eigenfunction of the whole system.

To constrain the excited state particle orbitals $|\varphi_A\rangle$ orthogonal to the ground state occupied orbitals $|\varphi_A^0\rangle$, we need $\langle \varphi_A | (1 - \rho_{\notin A}^0) | \varphi_A^0 \rangle = 0$. The following equation is solved with a Lagrange multiplier λ ,

$$\frac{\partial L}{\partial \langle \varphi_A |} = (1 - (1 - \rho_{\notin A}) | \varphi_A \rangle \langle \varphi_A |) (1 - \rho_{\notin A}^0) f (1 - \rho_{\notin A}^0) | \varphi_A \rangle - \lambda (1 - \rho_{\notin A}^0) | \varphi_A^0 \rangle = 0 \quad (53)$$

By multiplying $\langle \varphi_A^0 |$ on the left, the Lagrange multiplier λ can be obtained:

$$\lambda = \langle \varphi_A^0 | (1 - (1 - \rho_{\notin A}) |\varphi_A\rangle \langle \varphi_A|) (1 - \rho_{\notin A}) f (1 - \rho_{\notin A}) |\varphi_A\rangle \quad (54)$$

The equation then becomes,

$$\left(1 - \left(1 - \rho_{\notin A}^0\right) |\varphi_A^0\rangle \langle \varphi_A^0|\right) (1 - (1 - \rho_{\notin A}) |\varphi_A\rangle \langle \varphi_A|) (1 - \rho_{\notin A}) f (1 - \rho_{\notin A}) |\varphi_A\rangle = 0 \quad (55)$$

We can further rewrite the above equation into a symmetric form,

$$\rho' (1 - \rho_{\notin A}) f (1 - \rho_{\notin A}) \rho' |\varphi_i^A\rangle = \rho' (1 - \rho_{\notin A}) |\varphi_i^A\rangle \varepsilon_i^A \quad (56)$$

where $\rho' = 1 - \left(1 - \rho_{\notin A}^0\right) |\varphi_A^0\rangle \langle \varphi_A^0| = \left(1 - \rho_{\notin A}^0\right) |\varphi_{Av}^0\rangle \langle \varphi_{Av}^0|$ by using normalization property of complete non-orthogonal basis, $|\varphi_{Av}^0\rangle$ is ground state unoccupied orbitals. To solve this eigenequation, we multiply $\langle \varphi_{Av}^0 | = (\chi T_{Av}^0)^\dagger$ on the left and set $|\varphi_A\rangle = \chi T_A = \chi T_{Av}^0 T'_A$ to project the equation to ground state unoccupied orbitals space. The following equation is then obtained:

$$\left(T_{Av}^{0\dagger} F'_A T_{Av}^0\right) T'_A = \left(T_{Av}^{0\dagger} S'_A T_{Av}^0\right) T'_A E_A \quad (57)$$

After the diagonalization, the particle orbitals will be selected according to the order of ground state unoccupied orbitals.

Appendix B Derivation of a new approximate off-diagonal matrix element expression and its relation with previous results

According to the Kohn-Sham equation, we can obtain orthonormal Kohn-Sham (KS) wavefunction $|\Phi^{KS}\rangle$. Assume $|\Phi^{KS}\rangle$ is the wavefunction of DFT and H_t is the Hamiltonian

nian including correlation interaction. We can obtain $E_i^{DFT} = H_{ii}^{DFT} = \langle \Phi_i^{KS} | H_t | \Phi_i^{KS} \rangle$, $M_{ij} = \langle \Phi_i^{KS} | \Phi_j^{KS} \rangle$ and

$$H_{ii}^{DFT} = k_i^2 H_{ii}^{KS} = \langle k_i \Phi_i^{KS} | H | k_i \Phi_i^{KS} \rangle = \langle \Psi_i | H | \Psi_i \rangle \quad (58)$$

where $|\Psi_i\rangle = |k_i \Phi_i^{KS}\rangle$ and $k_i = \sqrt{H_{ii}^{DFT}/H_{ii}^{KS}}$. Similar as diagonal matrix element treatment, the off-diagonal matrix element can be denote as

$$H_{ij}^{DFT} = \langle \Phi_i^{KS} | H_t | \Phi_j^{KS} \rangle \approx \langle \Psi_i | H | \Psi_j \rangle = k_i k_j \langle \Phi_i^{KS} | H | \Phi_j^{KS} \rangle = \sqrt{\frac{H_{ii}^{DFT} H_{jj}^{DFT}}{H_{ii}^{KS} H_{jj}^{KS}}} H_{ij}^{KS} \quad (59)$$

Using first order Taylor approximation, we can obtain two previous expressions in Ref. 21,131.

$$\begin{aligned} H_{ij}^{DFT} &\approx \left(1 + \frac{H_{ii}^{DFT} - H_{ii}^{KS}}{2H_{ii}^{KS}}\right) \left(1 + \frac{H_{jj}^{DFT} - H_{jj}^{KS}}{2H_{jj}^{KS}}\right) H_{ij}^{KS} \\ &\approx H_{ij}^{KS} + \frac{H_{ij}^{KS}}{H_{ii}^{KS} + H_{jj}^{KS}} \left(H_{ii}^{DFT} + H_{jj}^{DFT} - H_{ii}^{KS} - H_{jj}^{KS}\right) \\ &\approx H_{ij}^{KS} + \frac{S_{ij}^{KS}}{2} \left(H_{ii}^{DFT} + H_{jj}^{DFT} - H_{ii}^{KS} - H_{jj}^{KS}\right) \end{aligned} \quad (60)$$

where $\frac{H_{ii}^{DFT} - H_{ii}^{KS}}{2H_{ii}^{KS}} \approx \frac{H_{ii}^{DFT} - H_{ii}^{KS}}{H_{ii}^{KS} + H_{jj}^{KS}}$, $\frac{H_{jj}^{DFT} - H_{jj}^{KS}}{2H_{jj}^{KS}} \approx \frac{H_{jj}^{DFT} - H_{jj}^{KS}}{H_{ii}^{KS} + H_{jj}^{KS}}$ and $H_{ij}^{KS} \approx \frac{S_{ij}^{KS}}{2} (H_{ii}^{KS} + H_{jj}^{KS})$ according to the extended Hückel theory (EHT).¹⁰⁶

References

- (1) Born, M.; Oppenheimer, R. *Ann. Phys.* **1927**, *389*, 457–484.
- (2) Cederbaum, L. S. In *Conical intersections: electronic structure, dynamics and spectroscopy*; Domcke, W., Yarkony, D. R., Köppel, H., Eds.; World Scientific, 2004; Vol. 15; p 3.
- (3) Köppel, H. In *Conical intersections: electronic structure, dynamics and spectroscopy*; Domcke, W., Yarkony, D. R., Köppel, H., Eds.; World Scientific, 2004; Vol. 15; p 175.

- (4) Baer, M. *Beyond Born-Oppenheimer: electronic nonadiabatic coupling terms and conical intersections*; John Wiley & Sons, 2006.
- (5) May, V.; Kühn, O. *Charge and Energy Transfer Dynamics in Molecular Systems*, 3rd ed.; Wiley-VCH: Weinheim, 2011.
- (6) Mead, C. A.; Truhlar, D. G. *J. Chem. Phys.* **1982**, *77*, 6090–6098.
- (7) Hsu, C.-P. *Acc. Chem. Res.* **2009**, *42*, 509–518.
- (8) You, Z.-Q.; Hsu, C.-P. *Int. J. Quantum Chem.* **2014**, *114*, 102–115.
- (9) Van Voorhis, T.; Kowalczyk, T.; Kaduk, B.; Wang, L.-P.; Cheng, C.-L.; Wu, Q. *Annu. Rev. Phys. Chem.* **2010**, *61*, 149–170.
- (10) Subotnik, J. E.; Yeganeh, S.; Cave, R. J.; Ratner, M. A. *J. Chem. Phys.* **2008**, *129*, 244101.
- (11) Bagus, P. S.; Schaefer III, H. F. *J. Chem. Phys.* **1972**, *56*, 224–226.
- (12) Broer, R.; Nieuwpoort, W. *J. Molec. Struct.: THEOCHEM* **1998**, *458*, 19–25.
- (13) Dederichs, P.; Blügel, S.; Zeller, R.; Akai, H. *Phys. Rev. Lett.* **1984**, *53*, 2512.
- (14) Wu, Q.; Van Voorhis, T. *Phys. Rev. A* **2005**, *72*, 024502.
- (15) Kaduk, B.; Kowalczyk, T.; Van Voorhis, T. *Chem. Rev.* **2012**, *112*, 321–370.
- (16) Yost, S. R. et al. *Nature Chem.* **2014**, *6*, 492–497.
- (17) Mavros, M. G.; Van Voorhis, T. *J. Chem. Phys.* **2015**, *143*, 231102.
- (18) Senatore, G.; Subbaswamy, K. *Phys. Rev. B* **1986**, *34*, 5754.
- (19) Wesolowski, T. A.; Warshel, A. *J. Phys. Chem.* **1993**, *97*, 8050–8053.
- (20) Jacob, C. R.; Neugebauer, J. *WIREs Comput Mol Sci* **2014**, *4*, 325–362.

- (21) Cembran, A.; Song, L.; Mo, Y.; Gao, J. *J. Chem. Theory Comput.* **2009**, *5*, 2702–2716.
- (22) Pauling, L. *The nature of the chemical bond and the structure of molecules and crystals: an introduction to modern structural chemistry*; Cornell university press, 1960; Vol. 18.
- (23) Shaik, S. S. *J. Am. Chem. Soc.* **1981**, *103*, 3692–3701.
- (24) Shaik, S. S.; Shurki, A. *Angew. Chem. Int. Ed.* **1999**, *38*, 586–625.
- (25) Shaik, S. S.; Hiberty, P. C. *A chemist's guide to valence bond theory*; John Wiley & Sons, 2007.
- (26) Song, L.; Gao, J. *J. Phys. Chem. A* **2008**, *112*, 12925–12935.
- (27) Cooper, D.; Gerratt, J.; Raimondi, M. *Adv. Chem. Phys.* **2009**, *69*, 319–397.
- (28) Goddard III, W. A.; Dunning Jr, T. H.; Hunt, W. J.; Hay, P. J. *Acc. Chem. Res.* **1973**, *6*, 368–376.
- (29) McWeeny, R. *Pure Appl. Chem.* **1989**, *61*, 2087–2101.
- (30) Van Lenthe, J.; Verbeek, J.; Pulay, P. *Mol. Phys.* **1991**, *73*, 1159–1170.
- (31) Song, L.; Song, J.; Mo, Y.; Wu, W. *J. Comput. Chem.* **2009**, *30*, 399–406.
- (32) Wu, W.; Su, P.; Shaik, S.; Hiberty, P. C. *Chem. Rev.* **2011**, *111*, 7557–7593.
- (33) Chen, Z.; Chen, X.; Wu, W. *J. Chem. Phys.* **2013**, *138*, 164119.
- (34) Mo, Y.; Gao, J. *J. Comput. Chem.* **2000**, *21*, 1458–1469.
- (35) Mo, Y.; Gao, J. *J. Phys. Chem. A* **2000**, *104*, 3012–3020.
- (36) Song, L.; Mo, Y.; Gao, J. *J. Chem. Theory Comput.* **2008**, *5*, 174–185.
- (37) Cembran, A.; Payaka, A.; Lin, Y.-l.; Xie, W.; Mo, Y.; Song, L.; Gao, J. *J. Chem. Theory Comput.* **2010**, *6*, 2242–2251.

- (38) Gao, J.; Cembran, A.; Mo, Y. *J. Chem. Theory Comput.* **2010**, *6*, 2402–2410.
- (39) Mo, Y.; Bao, P.; Gao, J. *Phys. Chem. Chem. Phys.* **2011**, *13*, 6760–6775.
- (40) Mo, Y.; Peyerimhoff, S. D. *J. Chem. Phys.* **1998**, *109*, 1687–1697.
- (41) Mo, Y.; Zhang, Y.; Gao, J. *J. Am. Chem. Soc.* **1999**, *121*, 5737–5742.
- (42) Mo, Y.; Gao, J.; Peyerimhoff, S. D. *J. Chem. Phys.* **2000**, *112*, 5530–5538.
- (43) Mo, Y.; Song, L.; Lin, Y. *J. Phys. Chem. A* **2007**, *111*, 8291–8301.
- (44) Stoll, H.; Wagenblast, G.; Preuß, H. *Theor. chim. Acta* **1980**, *57*, 169–178.
- (45) Gianinetti, E.; Raimondi, M.; Tornaghi, E. *Int. J. Quantum Chem.* **1996**, *60*, 157–166.
- (46) Gianinetti, E.; Vandoni, I.; Famulari, A.; Raimondi, M. *Adv. in Quant. Chem.* **1998**, *31*, 251–266.
- (47) Fornili, A.; Sironi, M.; Raimondi, M. *J. Molec. Struct.: THEOCHEM* **2003**, *632*, 157–172.
- (48) Nagata, T.; Takahashi, O.; Saito, K.; Iwata, S. *J. Chem. Phys.* **2001**, *115*, 3553–3560.
- (49) Ferenczy, G. G.; Adams, W. H. *J. Chem. Phys.* **2009**, *130*, 134108.
- (50) Khaliullin, R. Z.; Head-Gordon, M.; Bell, A. T. *J. Chem. Phys.* **2006**, *124*, 204105.
- (51) Khaliullin, R. Z.; Cobar, E. A.; Lochan, R. C.; Bell, A. T.; Head-Gordon, M. *J. Phys. Chem. A* **2007**, *111*, 8753–8765.
- (52) Smits, G. F.; Altona, C. *Theor. chim. Acta* **1985**, *67*, 461–475.
- (53) Couty, M.; Bayse, C. A.; Hall, M. B. *Theor. Chem. Acc.* **1997**, *97*, 96–109.
- (54) Sorakubo, K.; Yanai, T.; Nakayama, K.; Kamiya, M.; Nakano, H.; Hirao, K. *Theor. Chem. Acc.* **2003**, *110*, 328–337.

- (55) Mo, Y.; Song, L.; Lin, Y.; Liu, M.; Cao, Z.; Wu, W. *J. Chem. Theory Comput.* **2012**, *8*, 800–805.
- (56) Ren, H.; Provorse, M. R.; Bao, P.; Qu, Z.; Gao, J. *J. Phys. Chem. Lett.* **2016**, *7*, 2286–2293.
- (57) Chan, W.-L.; Berkelbach, T. C.; Provorse, M. R.; Monahan, N. R.; Tritsch, J. R.; Hybertsen, M. S.; Reichman, D. R.; Gao, J.; Zhu, X.-Y. *Acc. Chem. Res.* **2013**, *46*, 1321–1329.
- (58) You, Z.-Q.; Hsu, C.-P.; Fleming, G. R. *J. Chem. Phys.* **2006**, *124*, 044506.
- (59) Scholes, G. D.; Ghiggino, K. P. *J. Phys. Chem.* **1994**, *98*, 4580–4590.
- (60) Fujita, T.; Nakai, H.; Nakatsuji, H. *J. Chem. Phys.* **1996**, *104*, 2410–2417.
- (61) Runge, E.; Gross, E. K. *Phys. Rev. Lett.* **1984**, *52*, 997.
- (62) Ziegler, T.; Rauk, A.; Baerends, E. J. *Theor. chim. Acta* **1977**, *43*, 261–271.
- (63) Gilbert, A. T.; Besley, N. A.; Gill, P. M. *J. Phys. Chem. A* **2008**, *112*, 13164–13171.
- (64) Liu, J.; Zhang, Y.; Liu, W. *J. Chem. Theory Comput.* **2014**, *10*, 2436–2448.
- (65) Schmidt, M. W.; Baldridge, K. K.; Boatz, J. A.; Elbert, S. T.; Gordon, M. S.; Jensen, J. H.; Koseki, S.; Matsunaga, N.; Nguyen, K. A.; Su, S.; Windus, T. L.; Dupuis, M.; Montgomery, J. A. *J. Comput. Chem.* **1993**, *14*, 1347–1363.
- (66) Liu, D. C.; Nocedal, J. *Math. Prog.* **1989**, *45*, 503–528.
- (67) Nagata, T.; Iwata, S. *J. Chem. Phys.* **2004**, *120*, 3555–3562.
- (68) Famulari, A.; Calderoni, G.; Moroni, F.; Raimondi, M.; Karadakov, P. *J. Molec. Struct.: THEOCHEM* **2001**, *549*, 95–99.
- (69) Ferré, N.; Assfeld, X. *J. Chem. Phys.* **2002**, *117*, 4119–4125.

- (70) Gavnholt, J.; Olsen, T.; Englund, M.; Schiøtz, J. *Phys. Rev. B* **2008**, *78*, 075441.
- (71) Ziegler, T.; Seth, M.; Krykunov, M.; Autschbach, J.; Wang, F. *J. Chem. Phys.* **2009**, *130*, 154102.
- (72) De Mello, P. C.; Hehenberger, M.; Zernert, M. *Int. J. Quantum Chem.* **1982**, *21*, 251–258.
- (73) Glushkov, A.; Khetselius, O. Y.; Loboda, A.; Svinarenko, A.; Gurnitskaya, E.; Florko, T.; Sukharev, D.; Lovett, L. *Frontiers in Quantum Systems in Chemistry and Physics (Progress in Theoretical Chemistry and Physics vol 18)* ed S Wilson, PJ Grout, J Maruani, G Delgado-Barrio and P Piecuch. 2008.
- (74) Peng, B.; Van Kuiken, B. E.; Ding, F.; Li, X. *J. Chem. Theory Comput.* **2013**, *9*, 3933–3938.
- (75) Weeks, J. D.; Rice, S. A. *J. Chem. Phys.* **1968**, *49*, 2741–2755.
- (76) Huzinaga, S.; Cantu, A. *J. Chem. Phys.* **1971**, *55*, 5543–5549.
- (77) Surján, P. R. *Chem. Phys. Lett.* **2000**, *325*, 120–126.
- (78) Richings, G. W.; Karadakov, P. B. *Mol. Phys.* **2007**, *105*, 2363–2373.
- (79) Morokuma, K.; Iwata, S. *Chem. Phys. Lett.* **1972**, *16*, 192–197.
- (80) Tassi, M.; Theophilou, I.; Thanos, S. *Int. J. Quantum Chem.* **2013**, *113*, 690–693.
- (81) Tassi, M.; Theophilou, I.; Thanos, S. *J. Chem. Phys.* **2013**, *138*, 124107.
- (82) Theophilou, I.; Tassi, M.; Thanos, S. *J. Chem. Phys.* **2014**, *140*, 164102.
- (83) Evangelista, F. A.; Shushkov, P.; Tully, J. C. *J. Phys. Chem. A* **2013**, *117*, 7378–7392.
- (84) Derricotte, W. D.; Evangelista, F. A. *Phys. Chem. Chem. Phys.* **2015**, *17*, 14360–14374.

- (85) Broo, A.; Larsson, S. *Chem. Phys.* **1990**, *148*, 103–115.
- (86) Farazdel, A.; Dupuis, M.; Clementi, E.; Aviram, A. *J. Am. Chem. Soc.* **1990**, *112*, 4206–4214.
- (87) Broer, R.; Nieuwpoort, W. *Theor. chim. Acta* **1988**, *73*, 405–418.
- (88) Petsalakis, I. D.; Theodorakopoulos, G.; Nicolaides, C. A.; Buenker, R.; Peyrimhoff, S. *J. Chem. Phys.* **1984**, *81*, 3161–3167.
- (89) Löwdin, P.-O. *Phys. Rev.* **1955**, *97*, 1474.
- (90) Amos, A.; Hall, G. *Proc. R. Soc. Lond. Ser. A* **1961**, *263*, 483–493.
- (91) King, H. F.; Stanton, R. E.; Kim, H.; Wyatt, R. E.; Parr, R. G. *J. Chem. Phys.* **1967**, *47*, 1936–1941.
- (92) Speiser, S. *Chem. Rev.* **1996**, *96*, 1953–1976.
- (93) Holten, D.; Bocian, D. F.; Lindsey, J. S. *Acc. Chem. Res.* **2002**, *35*, 57–69.
- (94) Baldo, M. A.; O'Brien, D.; You, Y.; Shoustikov, A.; Sibley, S.; Thompson, M.; Forrest, S. *Nature* **1998**, *395*, 151–154.
- (95) Grätzel, M. *J. Photochem. Photobiol. C* **2003**, *4*, 145–153.
- (96) Mullen, K.; Scherf, U. *Organic light emitting devices*; Wiley-VCH, Weinheim, 2006.
- (97) Fleming, G. R.; van Grondelle, R. *Curr. Opin. Struct. Biol.* **1997**, *7*, 738–748.
- (98) van Grondelle, R.; Novoderezhkin, V. I. *Phys. Chem. Chem. Phys.* **2006**, *8*, 793–807.
- (99) Dirac, P. A. *Proc. R. Soc. Lond. Ser. A* **1927**, *114*, 243–265.
- (100) Hsu, C.-P.; You, Z.-Q.; Chen, H.-C. *J. Phys. Chem. C* **2008**, *112*, 1204–1212.

- (101) Harcourt, R. D.; Scholes, G. D.; Ghiggino, K. P. *J. Chem. Phys.* **1994**, *101*, 10521–10525.
- (102) Förster, T. *Ann. Phys.* **1948**, *437*, 55–75.
- (103) Scholes, G. D.; Harcourt, R. D.; Ghiggino, K. P. *J. Chem. Phys.* **1995**, *102*, 9574–9581.
- (104) Shi, B.; Gao, F.; Liang, W. *Chem. Phys.* **2012**, *394*, 56–63.
- (105) You, Z.-Q.; Hsu, C.-P. *J. Chem. Phys.* **2010**, *133*, 074105.
- (106) Hoffmann, R. *J. Chem. Phys.* **1963**, *39*, 1397–1412.
- (107) Troisi, A.; Orlandi, G. *J. Phys. Chem. B* **2002**, *106*, 2093–2101.
- (108) Cheung, D. L.; Troisi, A. *J. Phys. Chem. C* **2010**, *114*, 20479–20488.
- (109) Gajdos, F.; Valner, S.; Hoffmann, F.; Spencer, J.; Breuer, M.; Kubas, A.; Dupuis, M.; Blumberger, J. *J. Chem. Theory Comput.* **2014**, *10*, 4653–4660.
- (110) Kubas, A.; Gajdos, F.; Heck, A.; Oberhofer, H.; Elstner, M.; Blumberger, J. *Phys. Chem. Chem. Phys.* **2015**, *17*, 14342–14354.
- (111) Birks, J. B. *Rept. Prog. Phys.* **1975**, *38*, 903–974.
- (112) Azumi, S. P.; Tohrü; McGlynn *J. Chem. Phys.* **1964**, *41*, 3131.
- (113) Chandra, A.; Lim, E. *J. Chem. Phys.* **1968**, *49*, 5066–5072.
- (114) Kołaski, M.; Arunkumar, C. R.; Kim, K. S. *J. Chem. Theory Comput.* **2013**, *9*.
- (115) Shirai, S.; Iwata, S.; Tani, T.; Inagaki, S. *J. Phys. Chem. A* **2011**, *115*, 7687–7699.
- (116) Shirai, S.; Kurashige, Y.; Yanai, T. *J. Chem. Theory Comput.* **2016**, *12*, 2366–2372.
- (117) Förster, T. *Angew. Chem. Int. Ed.* **1969**, *8*, 333–343.

- (118) George, G.; Morris, G. *J. Molec. Spect.* **1968**, *26*, 67–71.
- (119) McConkey, J.; Trajmar, S.; Man, K.; Ratliff, J. *J. Phys. B: At. Mol. Phys.* **1992**, *25*, 2197.
- (120) Langelaar, J.; Rettschnick, R.; Lambooy, A.; Hoytink, G. *Chem. Phys. Lett.* **1968**, *1*, 609–612.
- (121) Takemura, T.; Aikawa, M.; Baba, H.; Shindo, Y. *J. Am. Chem. Soc.* **1976**, *98*, 2205–2210.
- (122) Lim, E. C. *Acc. Chem. Res.* **1987**, *20*, 8–17.
- (123) Pabst, M.; Lunkenheimer, B.; Köhn, A. *J. Phys. Chem. C* **2011**, *115*, 8335–8344.
- (124) Kim, D. *J. Phys. Chem. C* **2015**, *119*, 12690–12697.
- (125) Lewis, G. N.; Kasha, M. *J. Am. Chem. Soc.* **1944**, *66*, 2100–2116.
- (126) Kitaura, K.; Morokuma, K. *Int. J. Quantum Chem.* **1976**, *10*, 325–340.
- (127) Gao, J. *J. Phys. Chem. B* **1997**, *101*, 657–663.
- (128) Kitaura, K.; Ikeo, E.; Asada, T.; Nakano, T.; Uebayasi, M. *Chem. Phys. Lett.* **1999**, *313*, 701–706.
- (129) Bao, P.; Yu, Z.-H. *J. Comput. Chem.* **2011**, *32*, 248–259.
- (130) Bernstein, D. S. *Matrix mathematics: theory, facts, and formulas*; Princeton University Press, 2009.
- (131) Zhou, C.; Zhang, Y.; Gong, X.; Ying, F.; Su, P.; Wu, W. *J. Chem. Theory Comput.* **2017**, *13*, 627–634.